Computational Materials Science 45 (2009) 429–433

Contents lists available at ScienceDirect

Computational Materials Science

journal homepage: www.elsevier.com/locate/commatsci

Effect of water on brittle fracture of SiO_2 by molecular dynamics study

Q.H. Tang *

State Key Laboratory of Nonlinear Mechanics, Institute of Mechanics, Chinese Academy of Sciences, Beijing 100080, PR China

ARTICLE INFO

Article history:
Received 28 August 2008
Received in revised form 22 October 2008
Accepted 4 November 2008
Available online 23 December 2008

PACS::
62.20.Mk
62.20.Dc
68.10.Cr

Keywords:
Molecular dynamics simulation
Crack extension
Griffith theory
SiO_2
Water

ABSTRACT

The influence of water on the brittle behavior of β-cristobalite is studied by means of molecular dynamics (MD) simulation with the TTAM potential. Crack extension of mode I type is observed as the crack opening is filled up with water. The critical stress intensity factor K_{Ic}^{MD} is used to characterize the crack extension of MD simulation. The surface energy of SiO_2 covered with layers of water is calculated at temperature of 300 K. Based on the Griffith fracture criterion, the critical stress intensity factor $K_{Ic}^{Griffith}$ is calculated, and it is in good agreement with that of MD simulation.

1. Introduction

SiO_2 is a material widely used in microelectronic, semiconductor devices and biomedical engineering due to its many interesting properties on the different length scales. Many unusual silica nanostructures synthesized by a variety of methods [1–4] are required to be used in the water environment. In order to maintain a high surface integrity, water-based coolants are often used to ensure adequate heat dissipation in nano-machining processes such as nano-indentation and nano-scratching [5].

The topic of the crystal strength of bulk silica with the presence of water attracts many researchers. Griggs and Blacic [6] studied the strength of synthetic crystal, the result shows that water hydrolyzes the silicon–oxygen bonds and weakens the crystal strength. Leeuw et al. [7] employed computer modelling techniques to investigate the effect of water on the reactivity and stability of a SiO_2 nanotube and found that the surface of nanotube is relatively resistant to dissociative chemisorptions and silicon dissolution. This finding is important for modern application of nanostructures in fields ranging from catalysis to controlled release. Kalinichev and Kirkpatrick [8] have performed MD simulations to study the molecular-level structural and dynamical properties of water/α-quartz(0001) interfaces. Recently a number of studies were carried out on the chemical reactivity of silica–water interactions [9–11] based on ab initio calculation. They made a big progress and explained water to weaken Si–O bond from the view of atomic or electronic scale. Such a quantum-mechanical calculations are too expensive in computational cost and the classical MD simulations should have a role on investigation of mechanical properties of silica–water.

The motivation of this article is to study the effect of water on the crack extension of SiO_2. Both the MD simulation and the Griffith theoretical analysis are carried out to understand mechanism of crack extension.

2. Computation and modelling

2.1. Interatomic potential

It is known that the accuracy of MD simulations is dictated by the accuracy of the interatomic potentials being used. The interatomic potentials are available to model the different structures of silica. Most of them are empirical and are fitted to a wide variety of parameters in order to represent silica. Yoshitaka et al.[12] proposed an optimized Tersoff potential for Si/SiO_2 system based on force matching. Watanabe et al. [13] extend Stillinger–Weber potential of Si [14] to that of Si/O mixed system. Modified Tersoff potential and Stillinger–Weber potentials both have three-atom contributions and the computation process is very complex. TTAM

* Tel.: +86 01082543936; fax: +86 1082543977.
E-mail address: qhtang@lnm.imech.ac.cn.

0927-0256/$ - see front matter © 2008 Elsevier B.V. All rights reserved.
doi:10.1016/j.commatsci.2008.11.002

Table 1
Atomic interaction potential of TTAM, SiO_2.

SiO_2	Si–Si	TTAM [16]
	Si–O	
	O–O	

[15] and BKS [16] potentials are both the pair potentials and are widely accepted. Considering the computational efficiency, TTAM potential is used to describe interatomic interaction of SiO_2 in this article, see Table 1 and the parameters are listed in Table 2.

The simple point charge (SPC) model [17] of rigid water is usually used in MD exploring. SPC model use a total of three sites for the electrostatic interactions. Two hydrogen atoms are with the positive charges (Z_H = +0.41e) and an oxygen atom with the appropriate negative charge (Z_O = −0.82e). Inner a water molecule only the Coulomb electrostatic interactions are carried out between H–H and H–O, and there is no van der Waals interactions among them, see Table 3.

SPC model pointed out that as a water molecule interacts with other water molecule, the van der Waals interaction between two water molecules is computed using a Lennard–Jones (LJ) function with a single interaction point per water molecule centered on the oxygen atom O_w, and the Coulomb electrostatic interaction is also carried out between O_w–O_w, where O_w is the oxygen atom from H_2O and the representative of water molecule, see Table 3, and the parameters are listed in Table 4. There are no van der Waals interactions involving the hydrogen atoms between the water molecules due to the insignificant role of the hydrogen atoms among these interactions [17]. The same concept of per water molecule centered on the oxygen atom O_w is adopted for considering interaction between H_2O–SiO_2, it means that the interaction of H_2O–SiO_2 is equivalent to that of O_w–SiO_2 [18]. The interactions of O_w–Si and O_w–O_{silica} are computed by LJ function, but without considering the Coulomb electrostatic interaction between them, where O_{silica} is from SiO_2. The potentials of O_w–Si and O_w–O_{silica} are proved to be reliable in the MD studies by Tang and Zhang [18], and Zhang and Jiang [19]. The interaction potentials and parameters are listed in Tables 5 and 6.

Table 2
Potential parameters of SiO_2 in TTAM [16].

	Z	a (Å)	b (Å)	c (kcal$^{1/2}$ Å^3/mol$^{1/2}$)
Si	2.4e	0.8688	0.03285	23.18
O_{silica}	−1.2e	2.0474	0.17566	70.37

Table 3
Interactions inner H_2O and between H_2O–H_2O.

Inner H_2O	Z_O = 0.82e	O–H	Coulomb only
	Z_H = −0.41e	H–H	Coulomb only
H_2O–H_2O ⇔ O_w–O_w	Z_{Ow} = 0.82e	O_w–O_w	Coulomb + LJ

Table 4
Parameters of LJ potential between H_2O–H_2O, here H_2O ⇔ O_w [17].

Interatomic pair	Z	ϵ (kcal/mol)	δ (Å)
O_w–O_w	−0.82e	0.1553	3.166

Table 5
Interaction between H_2O–SiO_2 [17,18].

H_2O–SiO_2 ⇔ O_w–SiO_2	O_w–Si	LJ
	O_w–O_{silica}	LJ

Table 6
Parameters of LJ potential between H_2O–SiO_2, here H_2O ⇔ O_w [17,18].

Interatomic pair	ϵ (kcal/mol)	δ (Å)
O_w–O_{silica}	0.1553	3.166
O_w–Si	0.2218	3.388

The Ewald sum method is a technique for summing the interaction between an atom and all its periodic images along x, y, z directions. In this article, the periodic boundary condition is along y direction, and the fixed displacement boundary condition along x and z directions. As a test, the cutoff radius of 8 and 12 Å is taken to calculate the Coulomb electrostatic interaction, respectively, and the result shows that there is no some obvious difference between them. So the cutoff radius of 8 Å is taken to calculate the Coulomb electrostatic interaction instead of the Ewald sum method.

2.2. Elastic modulus of SiO_2

The modulus of silica is determined by the uniaxial extension of MD simulation at temperature of 300 K. The size of parallelepiped is of 29.2, 29.2 and 58.4 Å, about 3072 atoms. Both the strain and the stress are calculated. The stress is computed according to the formula given by Alber et al. [20].

$$\sigma_{kl} = \frac{1}{\Omega_0} \sum_{j,j \neq i} \frac{1}{2} \frac{\partial \phi(r)}{\partial r} \frac{r_{ij}^k r_{ij}^l}{r_{ij}} \tag{1}$$

where σ_{kl} is the stress component, r_{ij}^k and r_{ij}^l are k, l components of r_{ij}, Ω_0 is the volume of an atom.

The curve of stress σ versus strain ε is plotted in Fig. 1. Based on our calculation and isotropic continuum analysis, the elastic modulus is given $E = \frac{\sigma}{\varepsilon} = 300$ GPa, and Poisson ratio v is nearly zero which is similar to the result of Kimizuka and Kaburaki [21]. The shear modulus is $G = \frac{E}{2(1+v)} = 150$ GPa.

2.3. Model of crack

The parallelepiped with a slit is used as the simulation system and the sizes of x, y, and z directions are 233.6, 7.3 and 116.8 Å, respectively. The single edge crack is obtained by removing some atoms from the left side of block, and the length of crack is 60 Å and the width is 6 Å. The schematic diagrams are shown in Fig. 2.

Suppose that the simulation system is in the water environment. The periodic boundary condition is along the y direction, and the fixed displacement boundary condition along x and z directions. The method of a fixed displacement boundary condition was

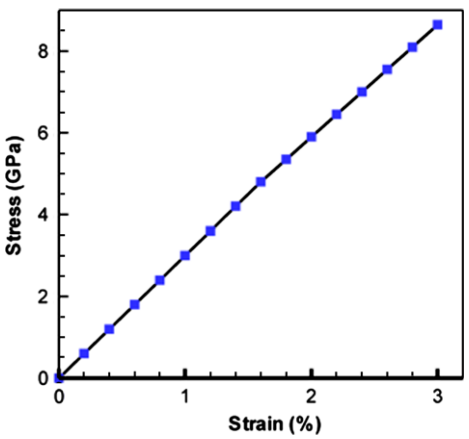

Fig. 1. Curve of stress versus strain.

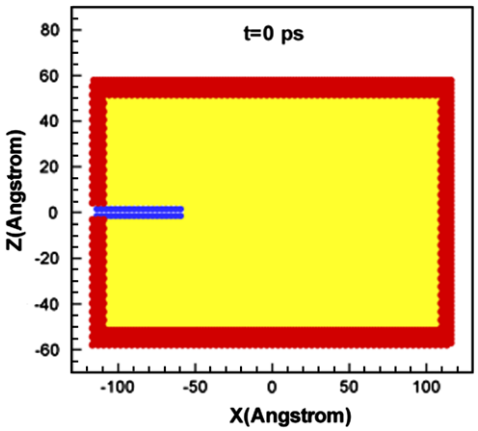

Fig. 2. Model of single edge crack, atom configuration at $t = 0$ ps.

described by DeCelis et al. [22] in detail. The displacements of atoms in boundary region are dictated by mode I with Ki field [23].

$$u_x = \frac{K_I}{4G}\sqrt{\frac{r}{2\pi}}((2\kappa - 1)\cos(\vartheta/2) - \cos(3\vartheta/2)) \quad (2)$$

$$u_z = \frac{K_I}{4G}\sqrt{\frac{r}{2\pi}}((2\kappa + 1)\sin(\vartheta/2) - \sin(3\vartheta/2)) \quad (3)$$

where $\kappa = 3 - 4v$, v is the Poisson's ratio. The stress intensity factor Ki is chosen as the loading parameter and the load rate is 0.02 M Pa $m^{1/2}$/fs and time step is 1 fs.

Our simulation is under the NVT ensemble. Initial velocities of atoms are specified based on the Maxwellian distribution corresponding to a given environment temperature, $T_0 = 300$ K, and the magnitudes may be adjusted so as to keep constant temperature in the system according to

$$v_i^{new} = \left\{\frac{3N\kappa_B T_0}{2}\left[\sum_{i=1}^{N}\frac{m_i(v_i^{old})^2}{2}\right]^{-1}\right\}^{1/2} v_i^{old} \quad (4)$$

where vi is the velocity of atom i, T_0 is a specified temperature, κ_B is Boltzmann's constant, and N is the number of atoms of the system in which the atoms in the fixed boundary region are excluded [24]. The time integration of motion is performed by the fifth Gear's predictor–corrector method [25].

3. Results and discussion

3.1. Analysis of molecular dynamics simulation

Two examples are considered. One is a crack opening filled up with water at $t = 0$ ps, without water added during the loading process; The other is the crack opening filled up with water continuously. The different results are obtained. For the first case, at $t = 81$ ps, the crack opening is up to a little more than 20 Å due to the applied load and interaction between water and crack surface. The effect of water on crack surface decreases with increase of crack opening. Fig. 3a shows that the micro-voids nucleate gradually near the crack tip. For the second case, at $t = 66$ ps, the crack opening is up to about 18 Å. At later times the crack opening is continuous to be filled up with water. Fig. 3b shows that near the crack tip the atoms are in the state of disorder. The failure of material SiO_2 accelerates crack extension. As the applied loading increases continuously, the

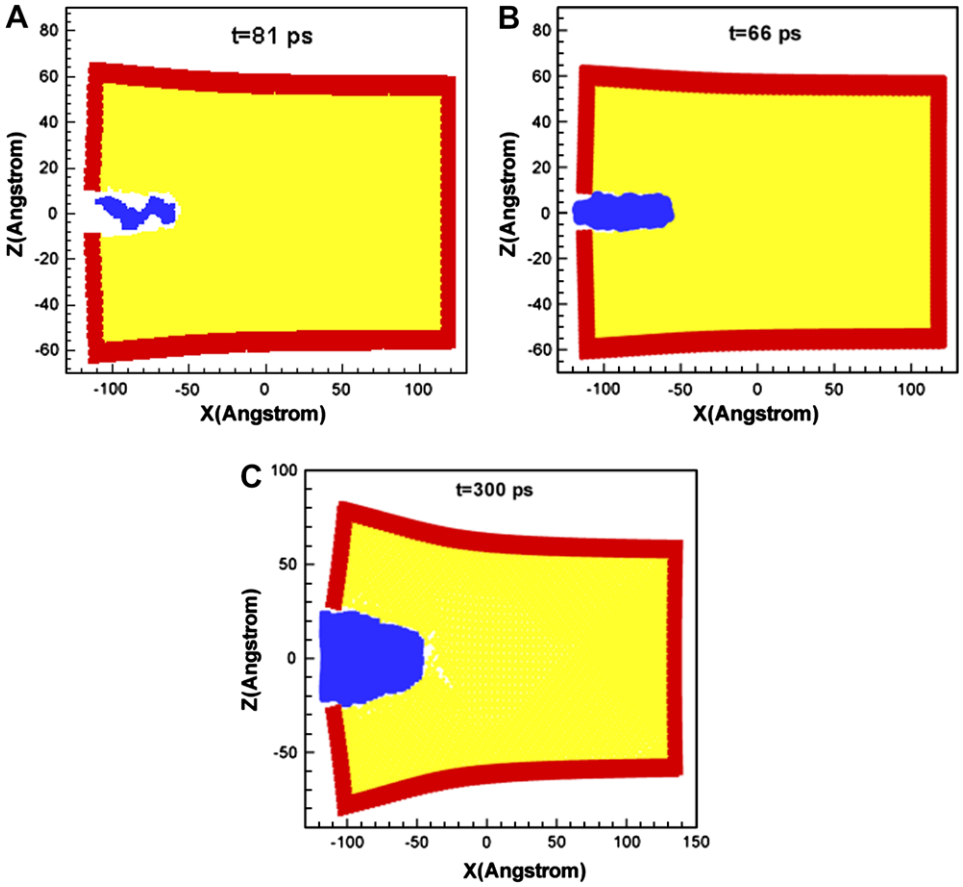

Fig. 3. Configuration evolutions of atom near crack tip: (a) $t = 81$ ps for case 1; (b) $t = 66$ ps for case 2 and (c) $t = 300$ ps for case 2.

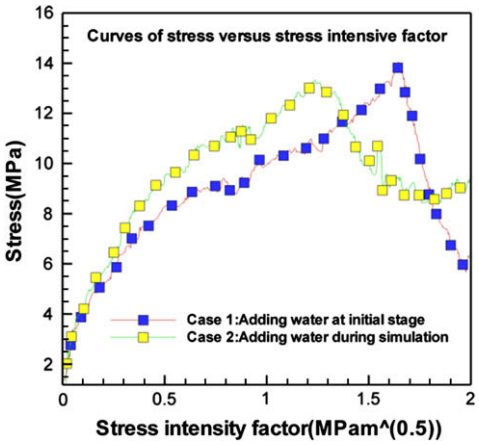

Fig. 4. Curves of stress versus stress intensity factor.

crack propagates. In the front of crack tip a lot of voids forming, growth and coalescence are observed because of the higher stress and strain around crack tip. When t = 300 ps, the crack extension by connection of voids and crack is displayed in Fig. 3c. The crack tip posited at −58 Å at the initial state in Fig. 2 is advanced to −45 Å. The results are similar to those of SiO_2 MD simulations by Brutzel et al. [26] and Muralidharan et al. [27]. And the branching crack nucleated in the front of main crack is also observed, it may be contributed by interaction between water and SiO_2.

The curves of stress versus the stress intensity factor are plotted in Fig. 4. For the first case, when t = 81 ps, the critical stress intensity factor K_{Ic}^{MD} is about 1.62 M Pa $m^{1/2}$, the stress is 13.4 GPa. After that time, as the applied load increases, the stress dropped suddenly, which means that crack extension occurs, and the evolution of atom configuration is plotted in Fig. 3a. For the second case, the critical state of crack extension is observed at t = 66 ps, the critical stress intensity factor is just about 1.32 M Pa $m^{1/2}$ and the stress is 13 GPa. For the same environment temperature of 300 K and the loading rate, the difference of simulation results of two cases is due to the interaction of the water molecules and the crack surface. Because water weakens the bond of Si–O–Si, the time of crack extension is advanced and the critical stress intensity factor and the maximum stress are reduced.

Griggs and Blacic [6] studied anomalous weakness of synthetic quartz crystals. The preferred explanation for this anomalous weakness is that this synthetic quartz contains water which hydrolyzed the silicon–oxygen bonds. In order to elucidate the mechanism of water-induced rupture of Si–O bond in silica, Michalske and Freiman [28] proposed a molecular model for the interaction of water with strained bonds in the glass at the tip of a crack, and the model can predict the effect of a given environment on crack growth. Watanabe et al. [13] investigated the structures and energies of complexes of Si–O bond interacting with water by using ab initio quantum mechanics calculation. The introduction of strain in the Si–O bond result in bending of the Si–O–Si angle and gradually leads to breakage of one Si–O bond.

3.2. Griffith's fracture theory

Michalske and Freiman [28] pointed out that their molecular model is consistent with the concept of Orowan. In 1944, Orowan [29] made a series of experiments to measure the surface energies of mica in the air and vacuum, respectively, and found that the surface energy in the air is less than that in the vacuum. Based on his experiments and the Griffith criteria (5) he suggested that the driving force for crack growth is the reduction in surface energy by the environment. Based on continuum mechanics Griffith [30] proposed the critical condition of crack extension $K_{Ic}^{Griffith}$, and it got a significant success in predicting the crack extension of the brittle materials.

$$K_{Ic}^{Griffith} = 2\sqrt{\frac{G\gamma_s}{1-\nu}} \tag{5}$$

where $K_{Ic}^{Griffith}$ is the critical stress intensity factor, G is the shear modulus, γ_s is the surface energy, and ν is the Poisson ratio.

The parallelepiped sample containing 12,288 atoms was selected for calculating the surface energy of SiO_2. The upper surface of sample is along the positive z direction and covered with a layer of water molecules. First, the total potential energy of system was calculated with the periodic boundary condition along x, y and z directions; then the potential energy of system was calculated with non-periodic boundary condition along z direction. The surface energy γ_s is given by

$$\gamma_s = \frac{\phi_2 - \phi_1}{2S_{xy}} \tag{6}$$

where S_{xy} is the area of plane xy. $\gamma_s^1 = 4.428$ J/m^2 for surface covered with a layer of water molecules and $\gamma_s^2 = 4.38$ J/m^2 with two layers of water molecules. The surface energy decreases with the increment of the layers of water molecules on the surface.

Substituting the shear modulus, the Poisson radio and the surface energies γ_s^1 and γ_s^2 into Eq. (5), the critical stress intensity factors are $K_{Ic}^{Griffith} = 1.7525$ M Pa $m^{1/2}$ and 1.621 M Pa $m^{1/2}$ for γ_s^1 and γ_s^2, respectively. According to the Griffith criterion of crack extension, when the stress intensity factor reaches $K_{Ic}^{Griffith}$, the crack begins to propagate. The result of Griffith theory is in good agreement with that of our MD simulation $K_{Ic}^{MD} = 1.62$ M Pa $m^{1/2}$ for the first case. And there is a little difference between $K_{Ic}^{Griffith}$ and K_{Ic}^{MD} of the second case, the difference is within 20%. Based on our calculation of the surface energy it can be induced that the difference will be reduced when surface is covered with many layers of water molecules.

4. Conclusion

Both MD simulation and the Griffith crack theory are carried out in order to understand the behavior of crack extension with the crack opening filled up with water. The interaction of water molecules and crack surfaces can weaken the strength of β-SiO_2. The critical stress intensity factor is used to characterize crack extension, K_{Ic}^{MD} is about 1.62 M Pa $m^{1/2}$ for the crack opening filled up with water at the initial stage; and 1.32 M Pa $m^{1/2}$ for the crack opening filled up with water continuously. The result of MD simulation shows that the effect of water on crack extension is obvious, and it is in good agreement with that of the Griffith fracture theory.

Acknowledgements

The research presented here was supported by the National Natural Science Foundation of China (Grant Nos. 10372107, 10721202, 10872197) and Chinese Academy of Sciences (Grant No. KJCX2-YW-M04), and Institute of Computational Mathematics, Chinese Academy of Sciences (CAS).

References

[1] N. Nishiyama, S. Tanaka, Y. Egashira, Y. Oku, K. Ueyama, Chem. Mater. 15 (2003) 1006–1011.
[2] M.P. Zach, J.T. Newberg, L. Sierra, J.C. Hemminger, R.M. Penner, J. Phys. Chem. B 107 (2003) 5393–5397.
[3] H.F. Zhang, C.M. Wang, E.C. Buck, L.S. Wang, Nano Lett. 3 (2003) 577.
[4] J.F. Bertone, J. Cizeron, R.K. Wahi, J.K. Bosworth, V.L. Colvin, Nano Lett. 3 (2003) 655.

[5] L.C. Zhang, I. Zarudi, Int. J. Mech. Sci. 43 (2001) 1985.
[6] D.T. Griggs, J.D. Blacic, Science 147 (1965) 292.
[7] N.H. Leeuw, D. Zhimei, L. Ju, Y. Sidney, T. Zhu, Nano Lett. 3 (2003) 1347.
[8] A.G. Kalinichev, R.J. Kirkpatrick, Geochim Cosmochim Acta 69 (2005) A510.
[9] J.D. Bene, K. Runge, R. Bartlett, Comput. Mater. Sci. 27 (2003) 102.
[10] M.H. Du, A. Kolchin, H.P. Cheng, J. Chem. Phys. 13 (2003) 6418.
[11] S.B. Trickey, S. Yip, H.P. Cheng, K. Runge, P.A. Deymier, J. Comput.-Aided Mater. Design 13 (2006) 1.
[12] U.T. Yoshitaka, D. Kazuyuki, H. Makoto, I. Tomio, Comput. Mater. Sci. 25 (2002) 447.
[13] T. Watanabe, H. Fujiwara, H. Noguchi, T. Hshino, I. Ohdemari, Jpn. J. Appl. Phys. 38 (1999) L366.
[14] F.H. Stillinger, T.A. Weber, Phys. Rev. B 31 (1985) 5262–5271.
[15] S. Tsuneyuki, M. Tsukada, H. Aoki, Phys. Rev. Lett. 61 (1988) 869.
[16] B.W.H. Van Beest, G.J. Kramer, Phys. Rev. Lett. 64 (1990) 1955.
[17] A.R. Leach, Molecular Modelling: Principles and Applications, Addison Wesley Longman, 1996.
[18] C.Y. Tang, L.C. Zhang, Nanotechnology 16 (2005) 15.
[19] L. Zhang, S. Jiang, J. Chem. Phys. 117 (2002) 1804.
[20] I. Alber, J.L. Bassani, et al., Philos. Trans. Roy. Soc. London A 339 (1992) 555.
[21] H. Kimizuka, H. Kaburaki, Phys. Stat. Sol. B 242 (2005) 607.
[22] B. DeCelis, A. Argon, S. Yip, J. Appl. Phys. 54 (1983) 4864.
[23] D. Broek, Elementary Engineering Fracture Mechanics, Noordhoff International Publishing, Leyden, 1974.
[24] W.C.D. Cheong, L.C. Zhang, Nanotechnology 11 (2000) 173–180.
[25] M.P. Allen, D.J. Tildesley, Computer Simulation of Liquid, Oxford University Press, New York, 2000. p. 340.
[26] L.V. Brutzel, C.L. Rountree, R.K. Kalia, A. Nakano, P. Vashishta, Mater. Res. Soc. Symp. Proc. 703 (2002) 117.
[27] K. Muralidharan, J.H. Simmons, P.A. Deymier, K. Runge, J. Non-Cryst. Solids 351 (2005) 1532.
[28] T.A. Michalske, S.W. Freiman, J. Am. Ceram. Soc. 66 (1944) 284.
[29] E. Orowan, Nature 154 (1944) 341.
[30] A.A. Griffith, Philos. Trans. Roy. Soc. A221 (1921) 163.